$$\sigma^2 = \langle d_{hkl}^{-4}\rangle - \langle d_{hkl}^{-2}\rangle^{-2} = \sum_{HKL} S_{HKL} h^H k^K l^L, \qquad (3.2.17)$$

where the sum is over terms with $H + K + L = 4$. This leads to a contribution to the width of a diffraction peak proportional to $\Gamma_{2\theta} = d^2\sqrt{\sigma^2}\tan\theta$ for angle-dispersive measurements, and $\Gamma_t = td^2\sqrt{\sigma^2}$ for time-of-flight neutron measurements. Strain broadening in real samples frequently leads to peak shapes that are closer to Lorentzian than Gaussian, and the justification of this expression breaks down because the second moment of the distribution of d^{-2} is then not defined. Nevertheless, this method is often successful at modelling the phenomenology of anisotropic peak broadening.

The parameters S_{HKL} arise from the nature of the strain and the values of elastic constants for any particular sample. Typically, they must therefore be regarded as phenomenological, and can be adjusted in fitting a model to observed data. They are constrained by the symmetry of the Laue group of the sample, which leads to restrictions on the S_{HKL} terms for the various Laue classes, listed in Table 3.2.1 (Popa, 1998).

Table 3.2.1
Restrictions and reflections of anisotropic strain parameters for the various Laue classes

$\bar{3}, \bar{3}m1, \bar{3}1m$: hexagonal indices.

Class	$\langle 1/d^2\rangle^2$
$\bar{1}$	$S_{400}h^4 + S_{040}k^4 + S_{004}l^4 + S_{220}h^2k^2 + S_{202}h^2l^2 + S_{022}k^2l^2 + S_{310}h^3k + S_{130}hl^3 + S_{301}h^3l + S_{103}hl^3 + S_{031}k^3l + S_{013}kl^3 + S_{211}h^2kl + S_{121}hk^2l + S_{112}hkl^2$
$2/m$ (b-axis unique)	$S_{400}h^4 + S_{040}k^4 + S_{004}l^4 + S_{220}h^2k^2 + S_{202}h^2l^2 + S_{022}k^2l^2 + S_{301}h^3l + S_{103}hl^3 + S_{121}hk^2l$
$2/mmm$	$S_{400}h^4 + S_{040}k^4 + S_{004}l^4 + S_{220}h^2k^2 + S_{202}h^2l^2 + S_{022}k^2l^2$
$4/m$	$S_{400}(h^4 + k^4) + S_{004}l^4 + S_{220}h^2k^2 + S_{202}(h^2 + k^2)l^2 + S_{310}(h^3k - hk^3)$
$4/mmm$	$S_{400}(h^4 + k^4) + S_{004}l^4 + S_{220}h^2k^2 + S_{202}(h^2 + k^2)l^2$
$\bar{3}$	$S_{400}(h^2 + k^2 + hk)^2 + S_{202}(h^2 + k^2 + hk)l^2 + S_{004}l^4 + S_{211}(h^3 - k^3 + 3h^2k)l + S_{121}(-h^3 + k^3 + 3hk^2)l$
$\bar{3}m1$	$S_{400}(h^2 + k^2 + hk)^2 + S_{202}(h^2 + k^2 + hk)l^2 + S_{004}l^4 + S_{301}(2h^3 + 3h^2k - 3hk^2 - 2k^3)l$
$\bar{3}1m$	$S_{400}(h^2 + k^2 + hk)^2 + S_{202}(h^2 + k^2 + hk)l^2 + S_{004}l^4 + S_{211}(h^2k + hk^2)l$
Hexagonal	$S_{400}(h^2 + k^2 + hk)^2 + S_{202}(h^2 + k^2 + hk)l^2 + S_{004}l^4$
Cubic	$S_{400}(h^4 + k^4 + l^4) + S_{220}(h^2k^2 + h^2l^2 + k^2l^2)$

3.2.3.5. *Preferred orientation (texture)*

The discussion of diffraction-peak intensities in Section 3.2.2.2 above presumes that the sample is a random powder, with every orientation equally probable. Real samples frequently exhibit some deviation from that ideal case, perhaps because of the way that grains of platy or acicular (needle-like) habit settle into a sample holder, or because a solid polycrystalline sample crystallized or grew anisotropically, or was formed or worked as a solid. The latter case is generally called texture, and can provide a fruitful basis for understanding the history or mechanical properties of a sample. The topic is further discussed in Chapter 5.3 of this volume. For the present purposes, deviation from a collection of randomly oriented grains will be regarded as an artifact to be minimized and/or modelled.

The distribution of orientations of crystallites in a sample can be studied using pole figures. For a given reflection **G**, the pole figure is defined as the probability density over a spherical surface that **G** falls in a particular direction relative to the sample. For a random powder, all pole figures would be uniform; for a single crystal, each pole figure would be a set of delta functions. Modelling of preferred orientation in the sample is accomplished by multiplying the theoretical intensity by the pole-figure density in the direction of the diffraction vector. Here we discuss two different treatments of preferred orientation.

The symmetrized spherical-harmonic approach follows Järvinen (1993), considering samples that are axially symmetric about some axis **P**. Experimentally, this can be ensured by rotating the sample about **P** during data collection. Take α to be the angle between **P** and the diffraction vector: α is zero for a conventional symmetrical flat plate and 90° for Debye–Scherrer geometry.

For a given reflection hkl, the polar-axis density in the diffraction direction may be expanded in spherical harmonics as

$$A(hkl, \alpha) = \sum_{ij} C_{ij} Y_{ij}(\theta_{hkl}, \varphi_{hkl}) P_i(\cos\alpha),$$

where Y_{ij} and P_i are the usual spherical harmonics and Legendre polynomials, and θ_{hkl} and φ_{hkl} are the spherical coordinates of the hkl reflection relative to some chosen axis of the crystal.

In general, there will be several reflections equivalent to hkl by the Laue symmetry of the crystalline phase, and so symmetry-adapted functions should replace the spherical harmonics in the above equation. Only even orders i are considered, because of the inversion symmetry of diffraction (neglecting imaginary atomic scattering amplitudes). The Laue symmetry of the crystalline phase implies that certain of the harmonics are zero; see the original article by Järvinen (1993) for explicit functional forms of the harmonics and a tabulation of which are allowed for each Laue group.

The second approach considered here is the widely used March (1932)–Dollase (1986) model, which is applicable to the most common powder-diffraction sample geometries of axial symmetry either along the diffraction vector or perpendicular to the diffraction plane, for samples whose preferred orientation arises from the settling of either disc- or rod-shaped crystallites in the sample holder. The cylinder axis **H** governs the preferred orientation. For any Bragg reflection **G**, the pole density in the diffraction direction is hypothesized to be a particular function of the angle α between **H** and **G**, *viz.*

$$A(G) = (R^2\cos^2\alpha + \sin^2\alpha/R)^{-3/2}.$$

Here R is a parameter describing the degree of preferred orientation; it is less than unity for maximum pole density at α = 0, *i.e.*, **H** ∥ **G**, as would be found for disc-like samples preferentially lying in the reflection plane. $R > 1$ corresponds to maximum pole density at $\alpha = 90°$, as might be found for acicular crystallites in either a flat-plate or Debye–Scherrer geometry. The particular functional form has some theoretical justification as a model for grain rotation in settling of a granular sample, as well as being properly normalized, suitable for oblate or prolate grains with a single parameter, and in agreement with pole distributions observed in many samples. To apply this model to powder-diffraction data, one must find the appropriate axis **H**, either through prior knowledge of growth habit or by trial and error.

3.2.3.6. *Extinction*

The analysis of diffracted intensities in this chapter has been premised on the assumption that the diffracted beam produced by each crystallite is much weaker than the incident beam, known

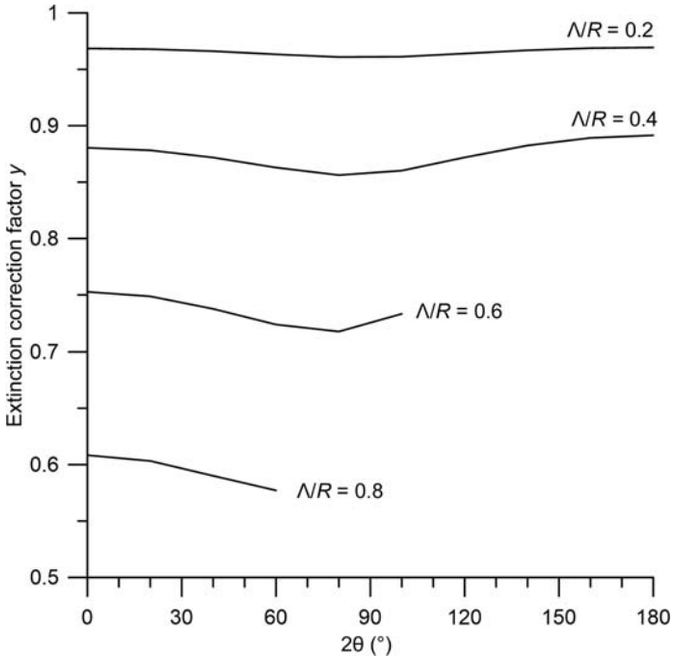

Figure 3.2.6
Extinction correction for spherical particles according to Thorkildsen & Larsen (1998).

as the kinematic approximation. This is a consequence of the Born approximation, whereby the diffracted intensity from one grain is proportional to the number of atoms within it. However, as the size of the crystallite grows, so will the intensity of the diffracted wave within it. The diffracted radiation will be re-diffracted back into the incident beam, leading to a measured integrated intensity less than the kinematic value, by a ratio $y(\mathbf{G}) = I_{\rm obs}(\mathbf{G})/I_{\rm kinematic}(\mathbf{G})$, which depends on the particular Bragg reflection **G**. This is the phenomenon of primary extinction, which can be understood within the framework of the dynamical theory of diffraction. The following discussion ignores absorption.

The relevant physical parameter is the extinction length Λ. For X-rays,

$$\Lambda(\mathbf{G}) = \frac{V}{r_e \lambda P |A_{\mathbf{G}}|},$$

where V is the unit-cell volume, $r_e = 2.82 \times 10^{-15}$ m, $A_{\mathbf{G}}$ is the structure factor, and P is the polarization factor: 1 or $\cos^2 2\theta$ for S or P polarization, respectively. For neutrons,

$$\Lambda(\mathbf{G}) = \frac{V}{\lambda |A_{\mathbf{G}}^{(n)}|}.$$

As an example, the 111 reflection of Si has an extinction length of 7.2 μm for 1.54 Å X-rays and 50 μm for 1.59 Å neutrons. Intensities from the kinematic theory are correct in the limit that the coherent grain size is much less than Λ. Note that extinction is most significant for the strongest reflections in a powder-diffraction pattern.

There are no exact calculations of extinction available for sample geometries applicable to powder samples, but Thorkildsen and Larsen have obtained a rigorous series solution for spherical particles of radius R in powers of Λ/R (Thorkildsen & Larsen, 1998). To lowest order,

$$y = 1 - (R/\Lambda)^2 f_1(\theta), \text{ where}$$
$$f_1(\theta) = \frac{8}{5\pi \sin 2\theta}(1 + \pi\theta - 4\theta^2 - \cos 4\theta - \theta \sin 4\theta) \text{ for } 0 \le \theta \le \pi/4$$
$$= \frac{4}{5\pi \sin 2\theta}(2 - \pi^2 + 6\pi\theta - 8\theta^2 - 2\cos 4\theta + \pi \sin 4\theta - 2\theta \sin 4\theta) \text{ for } \pi/4 \le \theta \le \pi/2.$$

This first term gives y accurate to 3% for $R/\Lambda \le 0.4$. Fig. 3.2.6 shows their calculated result up to fifth order.

3.2.4. The Debye scattering equation

The Debye scattering equation is an alternative method to compute the diffraction pattern of a collection of solid grains, which does not rely on a requirement of crystalline periodicity (Debye, 1915). Consequently, it is useful for cases where the grains of the sample are not fragments of idealized crystals, such as are frequently observed in nanoparticles. For a collection of identical grains, each containing N atoms having individual scattering amplitude b_j, $1 \le j \le N$, the orientation-average cross section per grain is given by

$$\left\langle \frac{{\rm d}\sigma}{{\rm d}\Omega} \right\rangle_{\rm orientation} = \sum_j^N b_j^2 + \sum_j^N \sum_{k \ne j}^N b_j b_k \frac{\sin(2\pi q r_{ij})}{2\pi q r_{ij}},$$

where r_{jk} is the distance between atoms j and k, and the scattering vector $q = 2\sin\theta/\lambda$. For neutrons, b_j is the scattering length; in the case of multiple isotopes of a given atomic species, one may use the coherent scattering length to obtain the coherent elastic cross section. For X-rays, $b_j = r_e f_j(\sin\theta/\lambda)$, the classical electron radius times the atomic scattering factor, and the cross section must be multiplied by the polarization factor as described in Section 3.2.2.2.1. This topic is treated in much greater detail in Chapters 3.6, 5.6 and 5.7 of this volume.

3.2.5. Summary

Although a powder-diffraction experiment is simple experimentally, considerable physics goes into determining the actual experimental data. Any user attempting to extract the maximum information from the diffraction data (especially through a Rietveld refinement) ultimately needs to understand all of the factors that affect the experimental data. This chapter provides a succinct summary of the major factors that contribute to the experimental data. Many of these factors are explored in more detail in other chapters of this volume.

References

Bindzus, N., Straasø, T., Wahlberg, N., Becker, J., Bjerg, L., Lock, N., Dippel, A.-C. & Iversen, B. B. (2014). *Experimental determination of core electron deformation in diamond*. *Acta Cryst.* A**70**, 39–48.
Brindley, G. W. (1945). *The effect of grain or particle size on x-ray reflections from mixed powders and alloys, considered in relation to the quantitative determination of crystalline substances by x-ray methods*. *Philos. Mag.* **36**, 347–369.
Caglioti, G., Paoletti, A. T. & Ricci, F. P. (1958). *Choice of collimators for a crystal spectrometer for neutron diffraction. Nucl. Instrum. Methods*, **3**, 223–228.
Caglioti, G., Paoletti, A. & Ricci, F. P. (1960). *On resolution and luminosity of a neutron diffraction spectrometer for single crystal analysis*. *Nucl. Instrum. Methods*, **9**, 195–198.
Cheary, R. W. & Coelho, A. (1992). *A fundamental parameters approach to X-ray line-profile fitting*. *J. Appl. Cryst.* **25**, 109–121.